Photospheric Current Spikes as Possible Predictors of Flares

Michael L. Goodman - NASA Marshall Space Flight Center/Jacobs ESSSA
(michael.l.goodman@nasa.gov)

Chiman Kwan, Bulent Ayhan & Eric L. Shang - Applied Research, LLC

2016 Conference on Partially Ionized Plasmas in Astrophysics: Aug.29 - Sept.2

JACOBS
ESSSA Group

Objective:

- **Are there enhancements in the photospheric J in NLRs of ARs that are useful for forecasting M/X flares?**
- **HMI: Full disk, continuous time coverage. $1''$, 12 minute resolution $\Rightarrow$ granulation dynamics is being resolved.**
- **Can HMI be used to detect hitherto undetected changes in J distribution?**

Approach:

- **Use HMI time series of photospheric $\mathbf{B}(x, y, t)$ to determine an analytic expression for $\mathbf{B}(x, y, z, t)$. Compute $\mathbf{J}, \mathbf{A}, \mathbf{E}$ in each pixel for 14 ARs. 7 with M/X flares. 7 with B, C, or no flares.**
- **Compute time series of $Q = \eta J^2$ (+ other quantities). Are there correlations with flare occurrence times?**

Magnetic Field

$$\mathbf{B}(x,y,z,t) = e^{-z/L(x,y,t)} \sum_{n=0}^{N_x} \sum_{m=0}^{N_y} \mathbf{b}_{nm}(t) e^{2\pi i \left(\frac{nx}{L_x} + \frac{my}{L_y}\right)}. \tag{1}$$

$L(x,y,t) = L_0(x,y,t) + zL_1(x,y,t)/L_0$, determined by the HMI data and the $\nabla \cdot \mathbf{B} = 0$ condition. No force-free assumption.

Vector Potential, Electric Field, Ohm's Law

Solve $\mathbf{A} = \nabla \times \mathbf{B}$, $\nabla \cdot \mathbf{A} = 0$ analytically. Then

$$\mathbf{E} = \frac{1}{c}\frac{\partial \mathbf{A}}{\partial t} - \nabla\phi \sim \frac{1}{c}\frac{\partial \mathbf{A}}{\partial t}. \tag{2}$$

Ohm's law: $\mathbf{E} + (\mathbf{V} \times \mathbf{B})/c = \eta \mathbf{J}$.

Solution Steps:

1. **Filter out the 6, 12, and 24 hour periods in the time series of $\mathbf{B}_{HMI}$ for each pixel. Corrects for spurious Doppler periods induced by SDO motion.**

2. **Set $\mathbf{B}(x, y, 0, t) = \mathbf{B}_{HMI}(x, y, t)$. Use FFT to solve for the $\mathbf{b}_{nm}(t)$.**

3. **Set $\nabla \cdot \mathbf{B}(x, y, z, t) = 0$. Expand in z, solve for $L(x, y, t)$.**

4. **Determine NLR(t) of each AR using Schrijver's algorithm (2007, ApJ).**

5. **At each time, compute the pixel and NLR integrated values of $Q, \mathbf{J} \cdot \mathbf{E}$, and $R_{CM} \equiv \mathbf{V} \cdot (\mathbf{J} \times \mathbf{B})/c$.**
   $\mathbf{J} \cdot \mathbf{E} = Q + R_{CM}$ (EM, CM KE, and thermal energy balance).
   Convection driven heating: $Q \sim -R_{CM}$ (i.e. $|\mathbf{J} \cdot \mathbf{E}|/Q \ll 1$).

6. **Compute power spectra, spectrograms, and cumulative distribution functions (CDFs) of time series of Q. Look for non-random structure.**

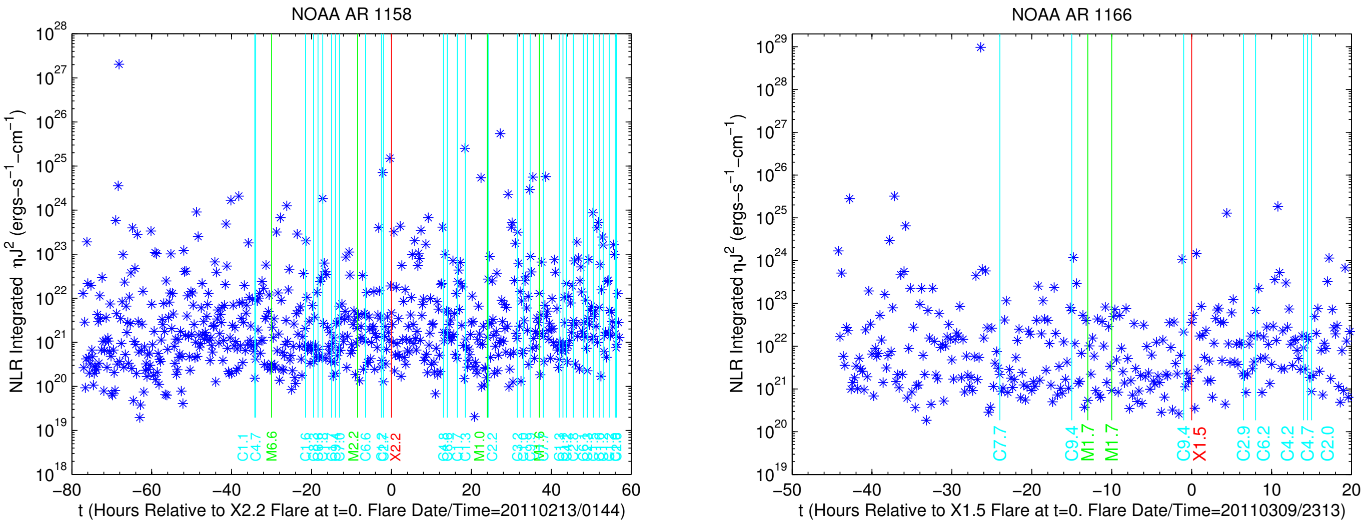

Figure 1: NLR integrated Q for 2 of 7 SF ARs.

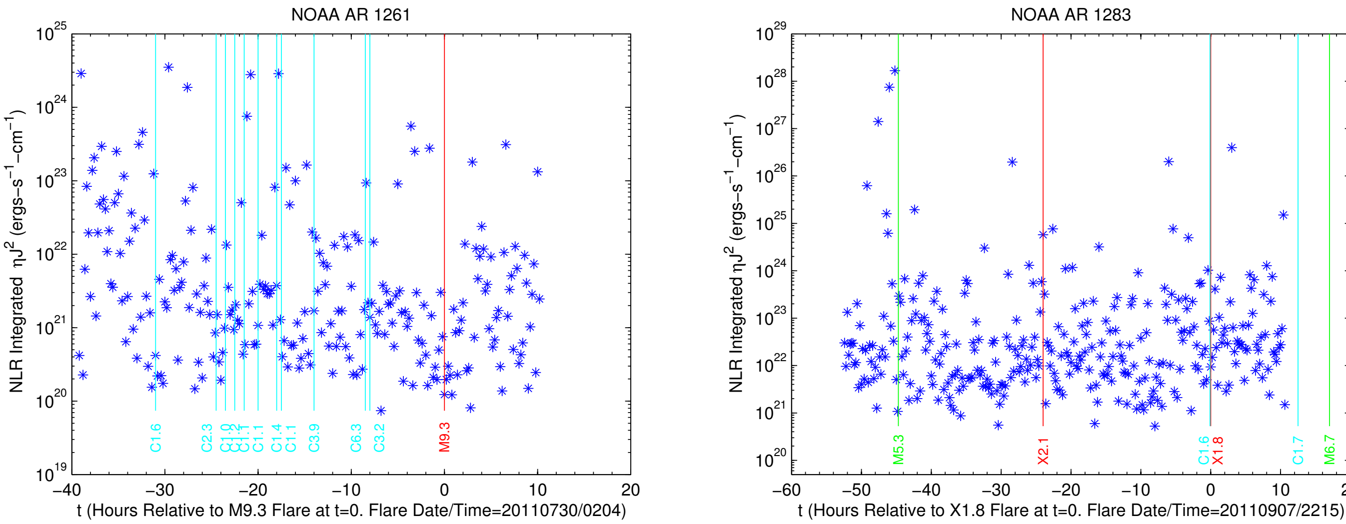

Figure 2: NLR integrated Q for 2 of 7 SF ARs.

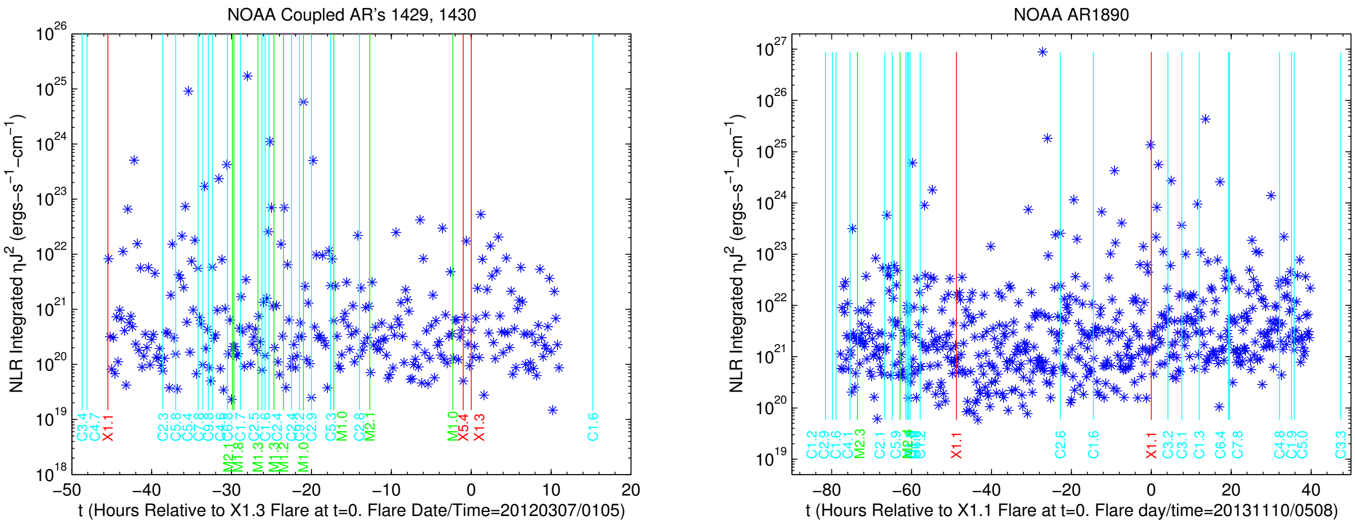

Figure 3: NLR integrated Q for 2 of 7 SF ARs.

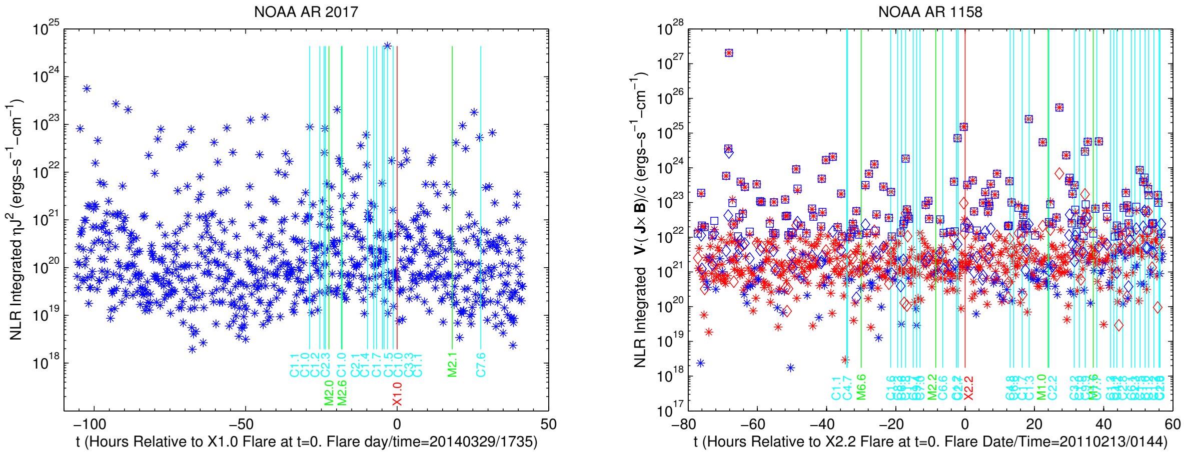

Figure 4: NLR integrated Q for the 7th SF AR, and R_{CM} for 1 of 7 SF ARs. Stars, Squares, Diamonds label values of RCM, Q, and $\mathbf{J} \cdot \mathbf{E}$. Blue/Red indicates positive/negative values. Q and $\mathbf{J} \cdot \mathbf{E}$ are plotted with RCM when the integrated $Q \geq 10^{22}$ ergs-cm^{-1}-s^{-1}.

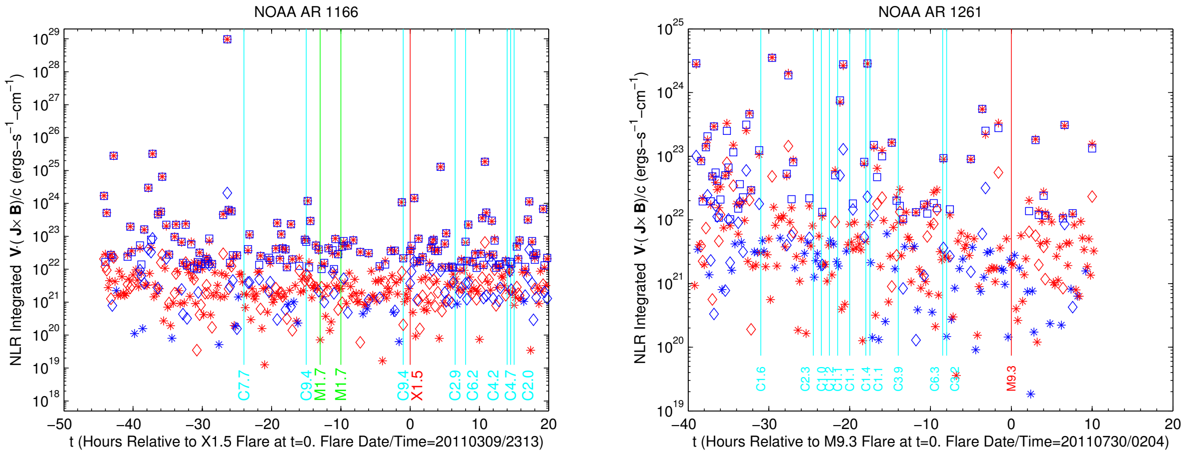

Figure 5: NLR integrated R_{CM} for 2 of 7 SF ARs. Stars, Squares, Diamonds label values of RCM, Q, and $\mathbf{J} \cdot \mathbf{E}$. Blue/Red indicates positive/negative values. Q and $\mathbf{J} \cdot \mathbf{E}$ are plotted with RCM when the integrated $Q \geq 10^{22}$ ergs-cm^{-1}-s^{-1}.

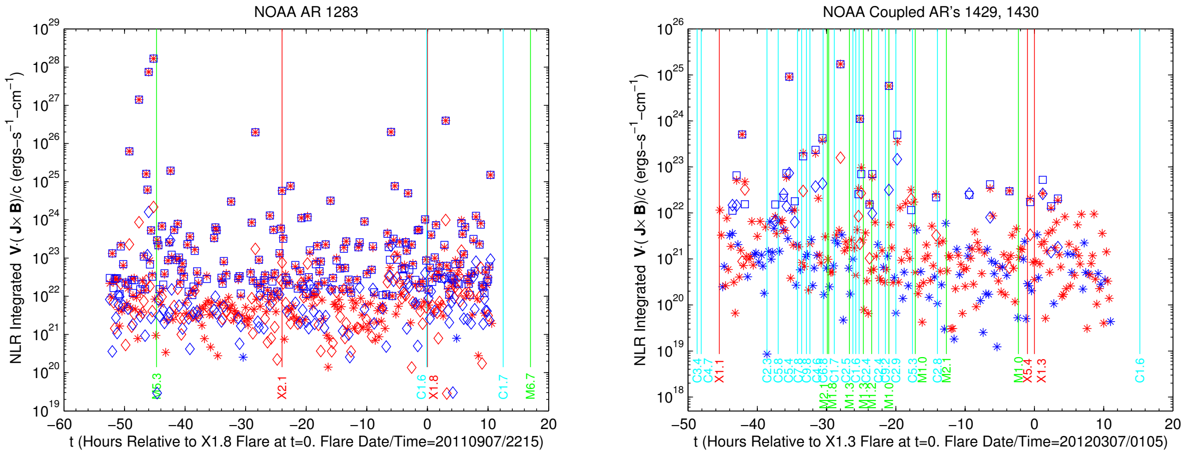

Figure 6: NLR integrated R_{CM} for 2 of 7 SF ARs. Stars, Squares, Diamonds label values of RCM, Q, and $\mathbf{J}\cdot\mathbf{E}$. Blue/Red indicates positive/negative values. Q and $\mathbf{J}\cdot\mathbf{E}$ are plotted with RCM when the integrated $Q \geq 10^{22}$ ergs-cm^{-1}-s^{-1}.

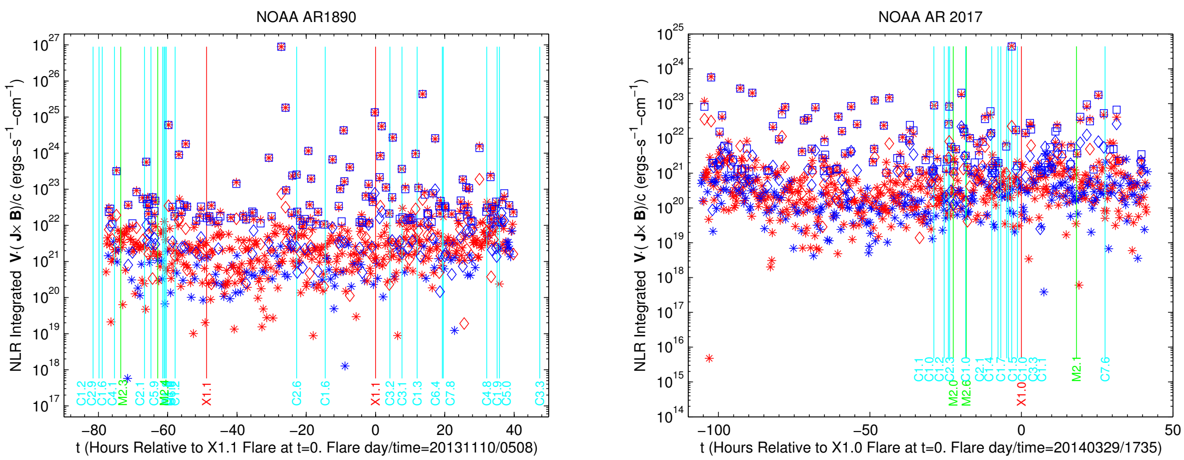

Figure 7: NLR integrated R_{CM} for 2 of 7 SF ARs. Stars, Squares, Diamonds label values of R_{CM}, Q, and $\mathbf{J} \cdot \mathbf{E}$. Blue/Red indicates positive/negative values. Q and $\mathbf{J} \cdot \mathbf{E}$ are plotted when the integral of $Q \geq 10^{22}(10^{21})$ ergs-cm^{-1}-s^{-1} for the left(right) plot.

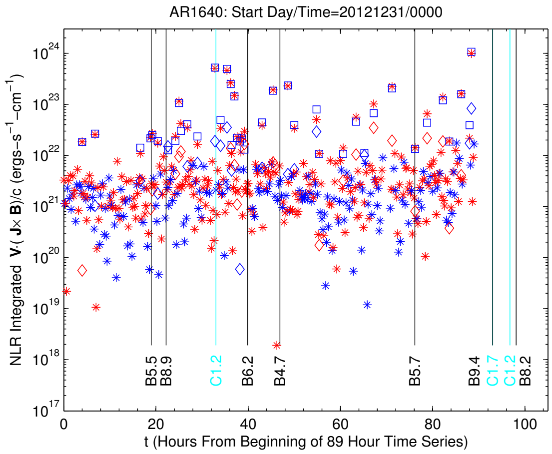

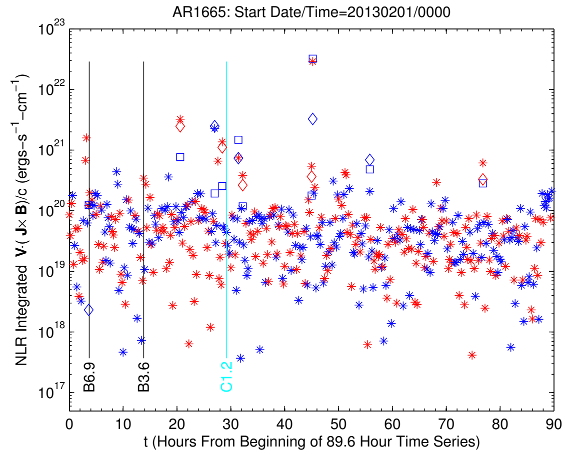

Figure 8: NLR integrated R_{CM} for 2 of 7 C ARs. Stars, Squares, Diamonds label values of R_{CM}, Q, and $\mathbf{J} \cdot \mathbf{E}$. Blue/Red indicates positive/negative values. Q and $\mathbf{J} \cdot \mathbf{E}$ are plotted when the integral of $Q \geq 10^{20}$ and 10^{22} ergs-cm^{-1}-s^{-1} for ARs 1665 and 1640.

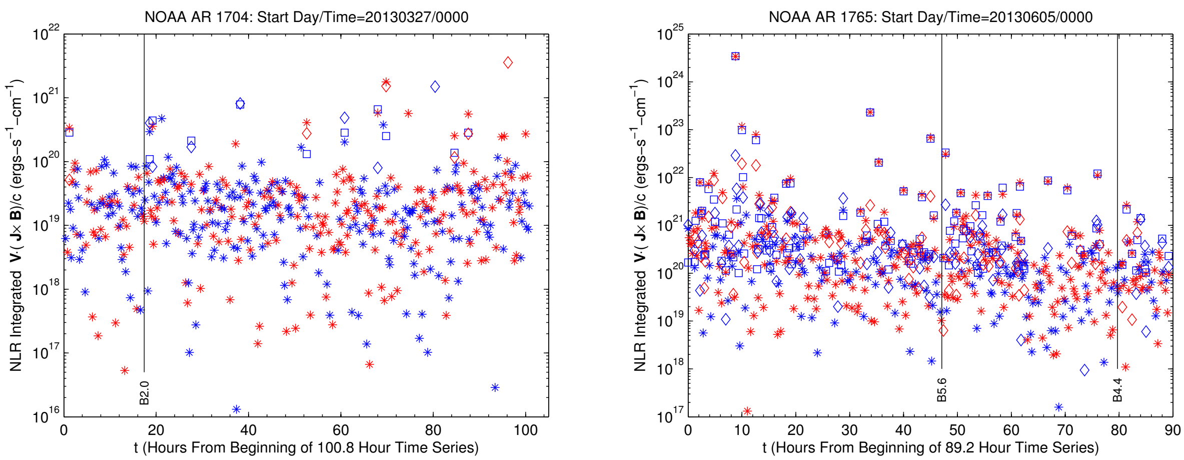

Figure 9: NLR integrated R_{CM} for 2 of 7 C ARs. Stars, Squares, Diamonds label values of R_{CM}, Q, and $\mathbf{J} \cdot \mathbf{E}$. Blue/Red indicates positive/negative values. Q and $\mathbf{J} \cdot \mathbf{E}$ are plotted when the integral of $Q \geq 10^{20}$ ergs-cm^{-1}-s^{-1}.

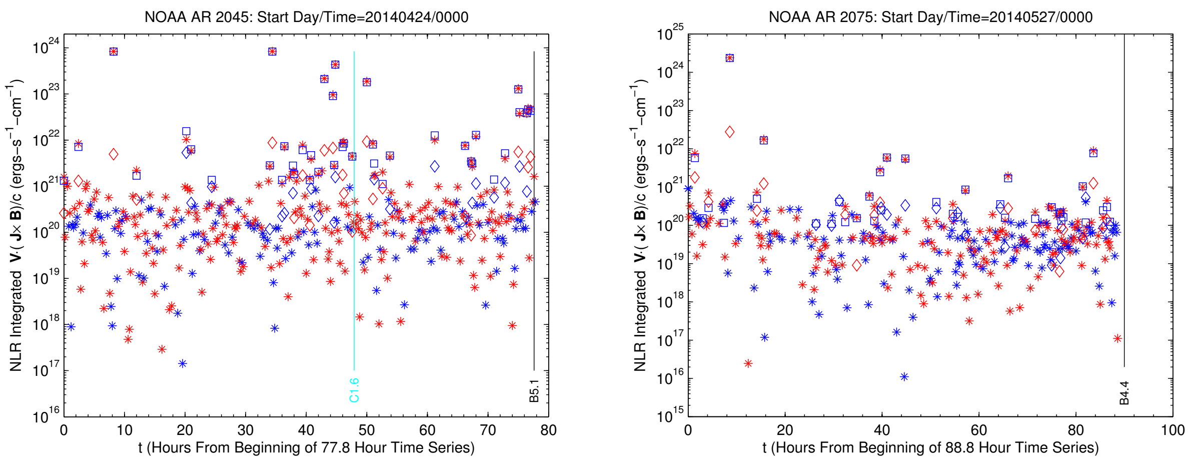

Figure 10: NLR integrated R_{CM} for 2 of 7 C ARs. Stars, Squares, Diamonds label values of R_{CM}, Q, and $\mathbf{J} \cdot \mathbf{E}$. Blue/Red indicates positive/negative values. Q and $\mathbf{J} \cdot \mathbf{E}$ are plotted when the integral of $Q \geq 10^{20}$ and 10^{21} ergs-cm^{-1}-s^{-1} for ARs 2075 and 2045.

Non-Random Structure in Time Series of Q:

- **Power Spectra: Sharp decreases in power at certain frequencies. In some cases by orders of magnitude.**
- **Spectrograms: Periodic intensity variations with respect to frequency at certain times, by orders of magnitude.**
- **Cumulative Distribution Functions: Scale invariant behavior of Q. $N(Q) = AQ^{-S}(S > 0)$ above threshold, and over a range of several orders of magnitude. Transition to SOC state above Q threshold?**
- **In almost all cases, clear that Q is not noise.**

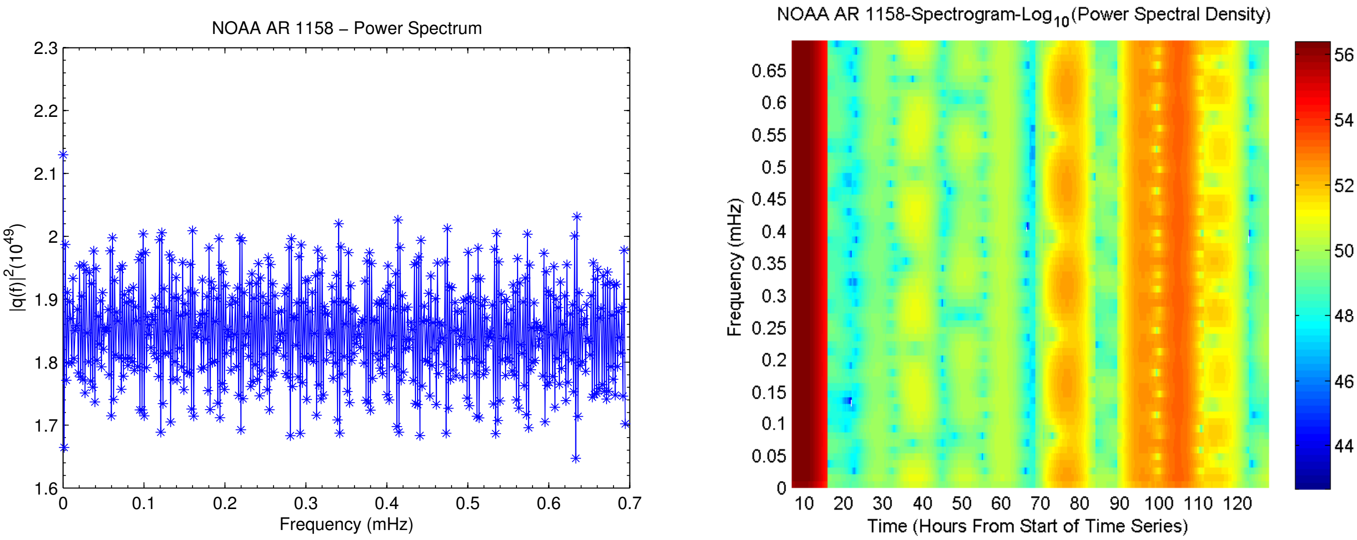

Figure 11: Power Spectrum and Spectrogram for SF AR 1158. (1 hr → 0.28 mHz)

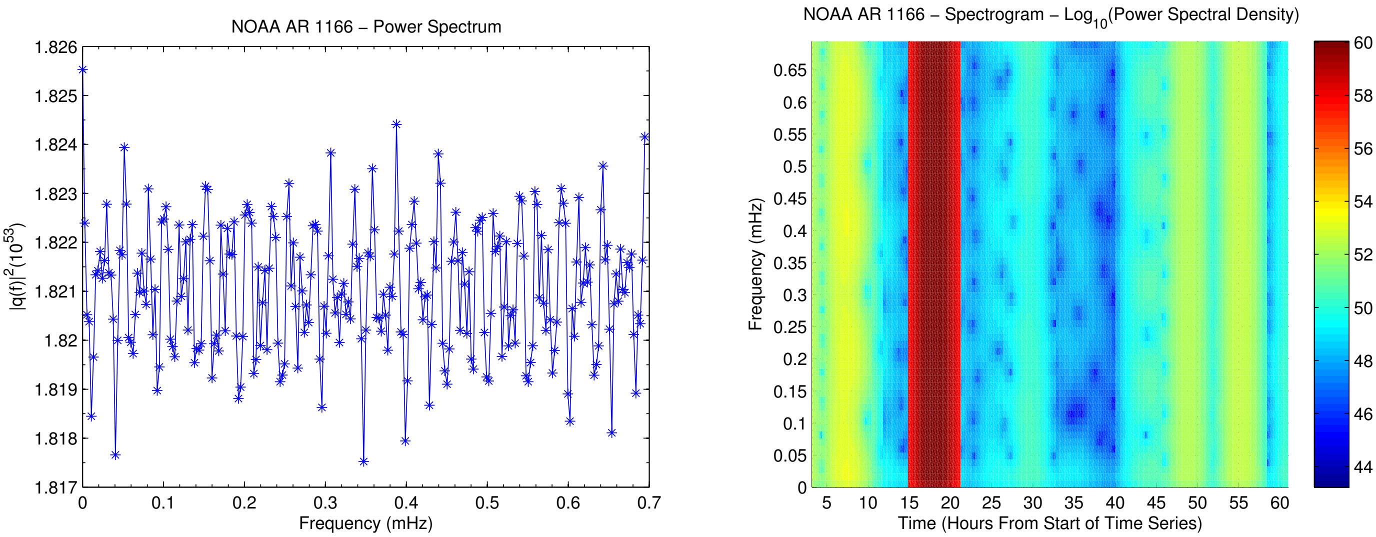

Figure 12: Power Spectrum and Spectrogram for SF AR 1166

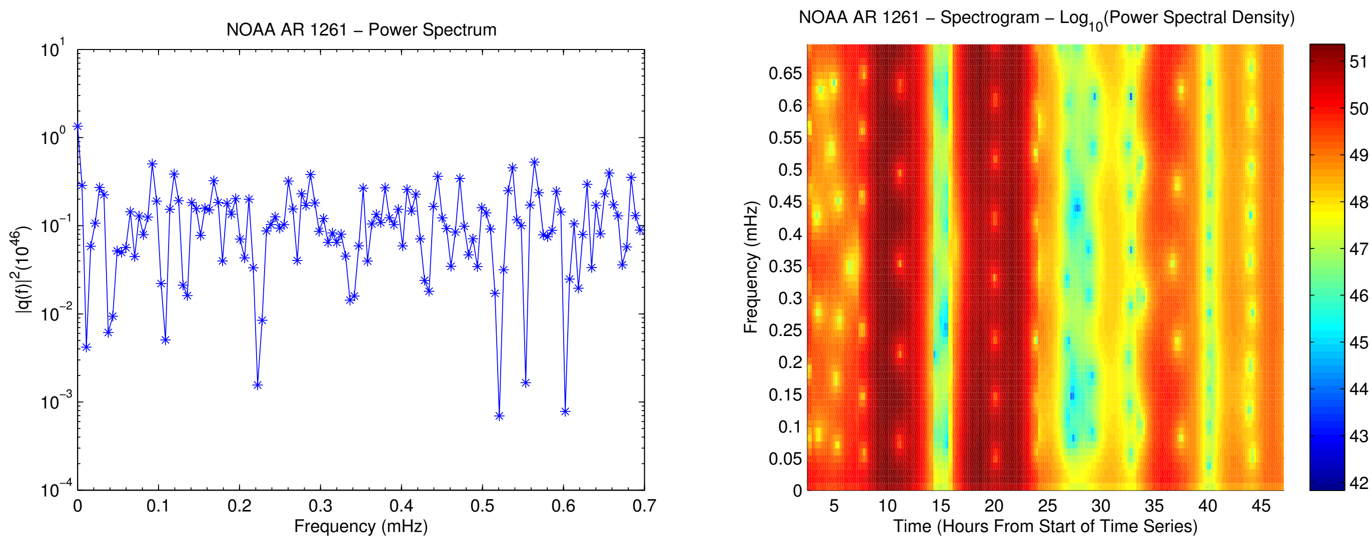

Figure 13: Power Spectrum and Spectrogram for SF AR 1261

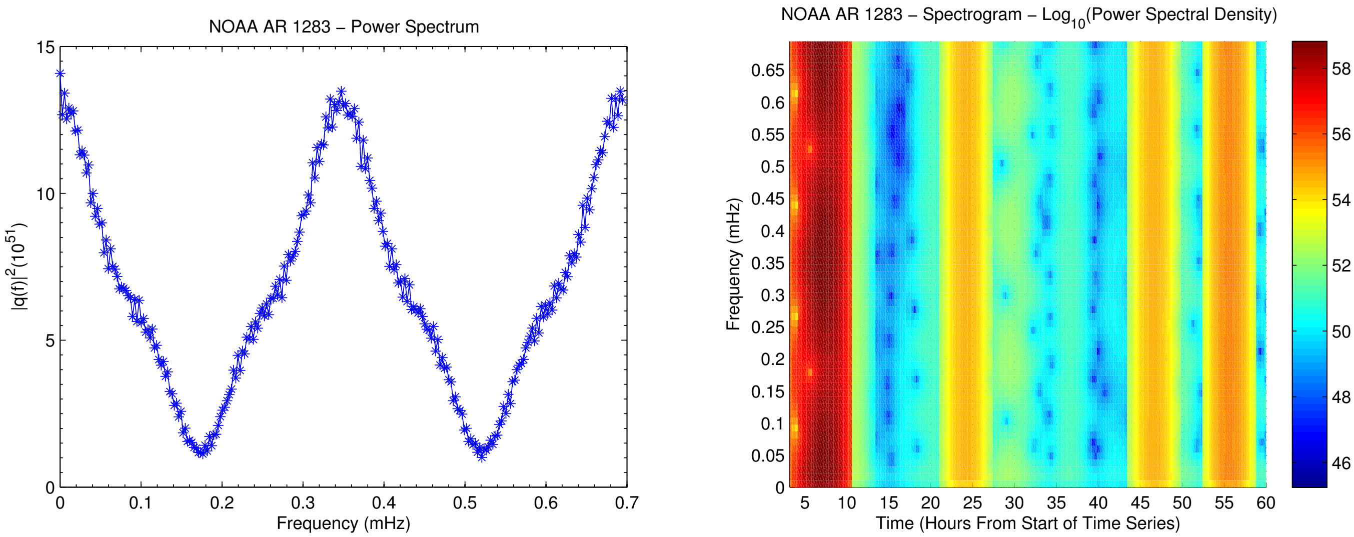

Figure 14: Power Spectrum and Spectrogram for SF AR 1158

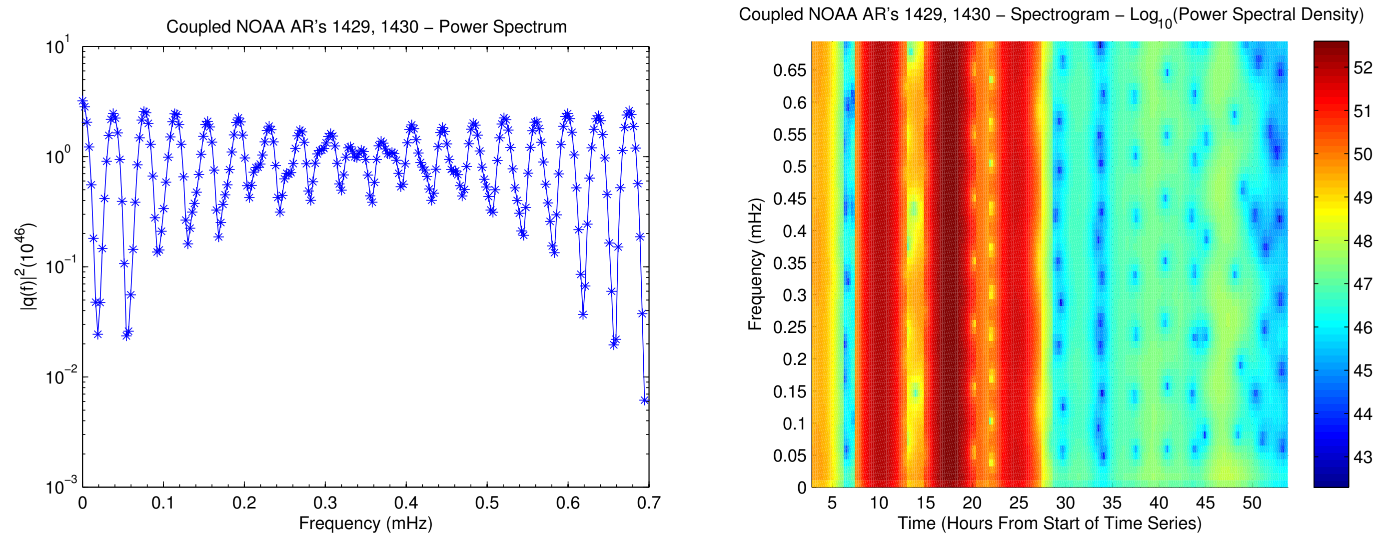

Figure 15: Power Spectrum and Spectrogram for SF AR 1429/1430

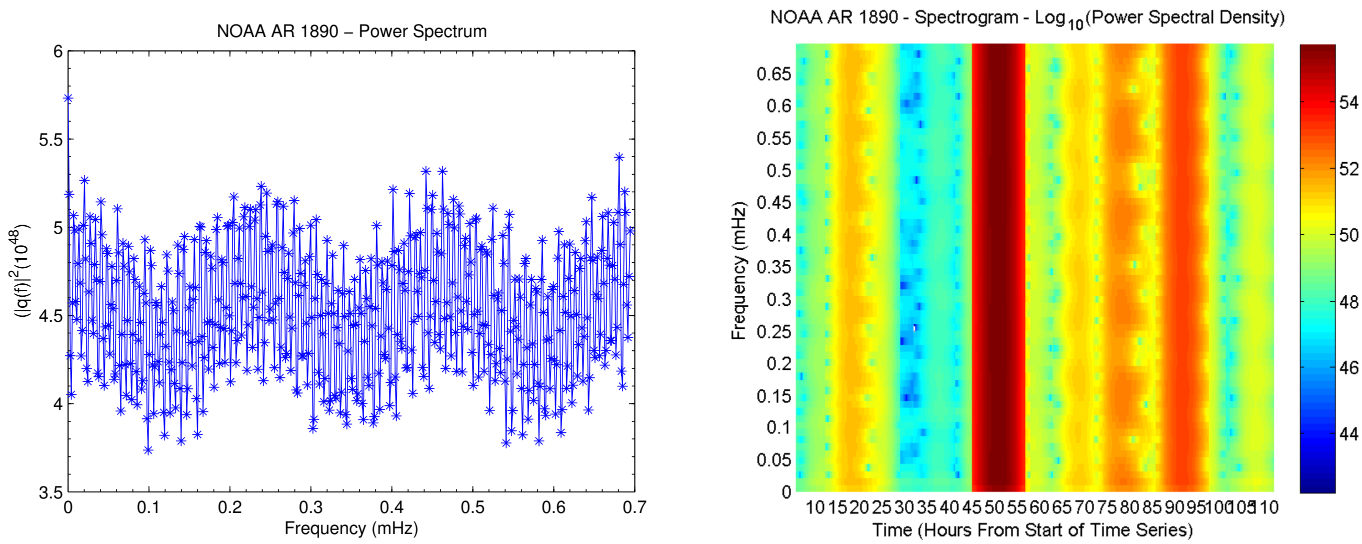

Figure 16: Power Spectrum and Spectrogram for SF AR 1890

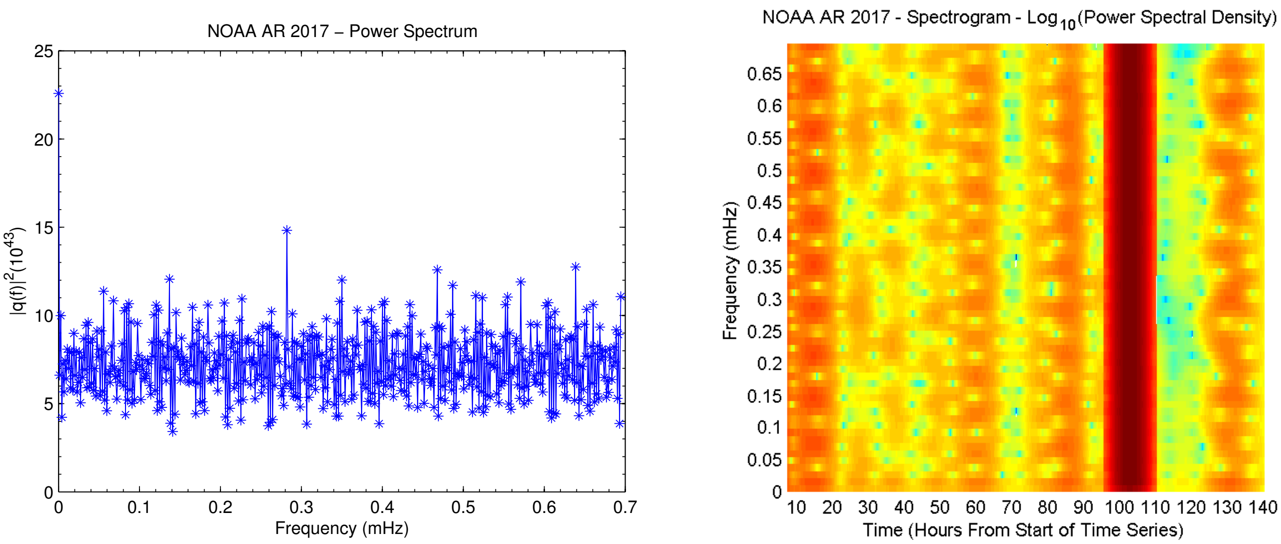

Figure 17: Power Spectrum and Spectrogram for SF AR 2017

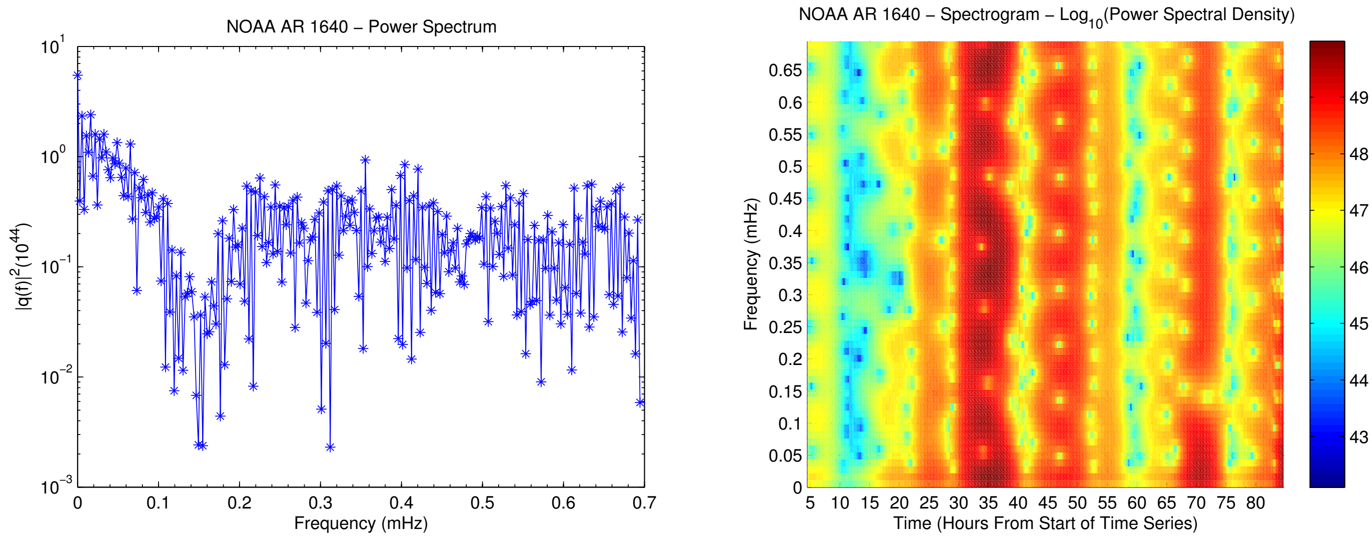

Figure 18: Power Spectrum and Spectrogram for C AR 1640

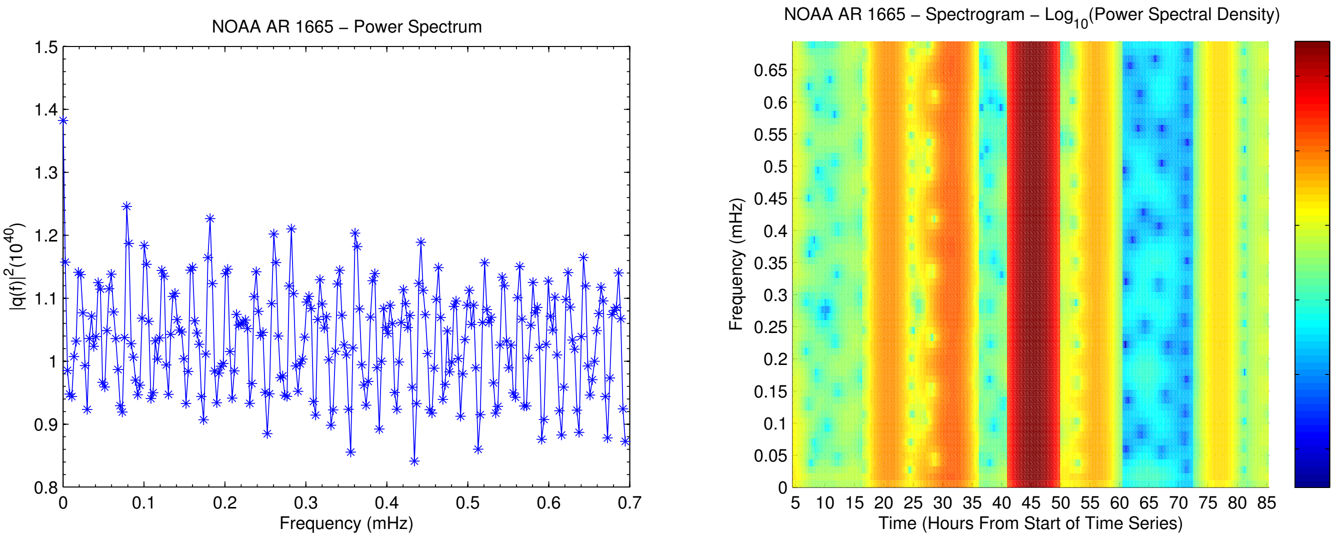

Figure 19: Power Spectrum and Spectrogram for SF AR 1665

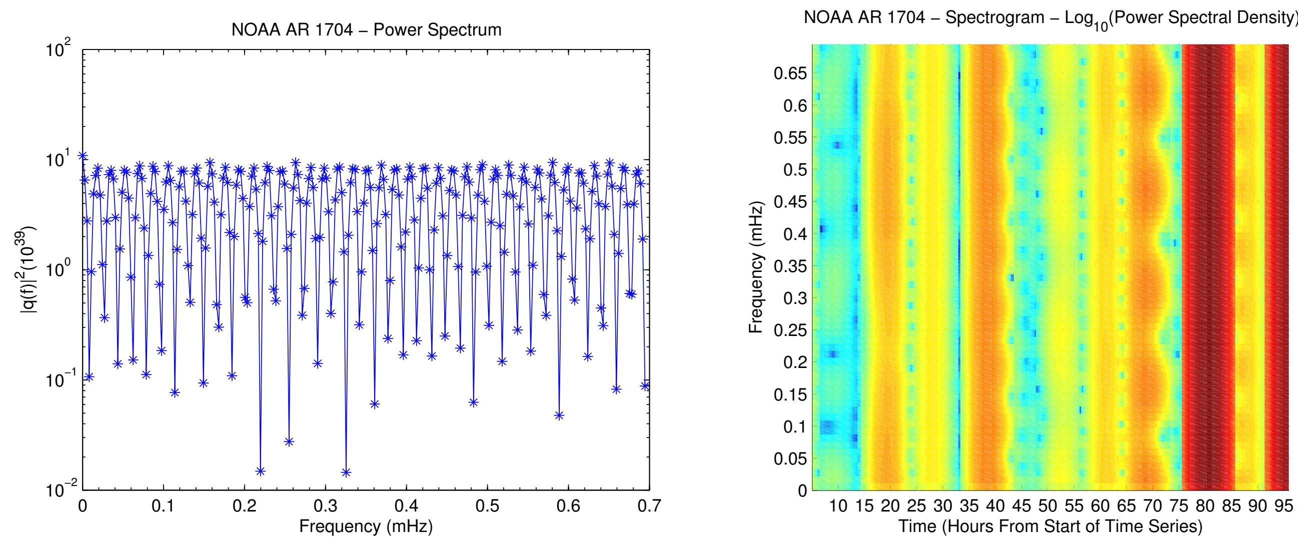

Figure 20: Power Spectrum and Spectrogram for C AR 1704

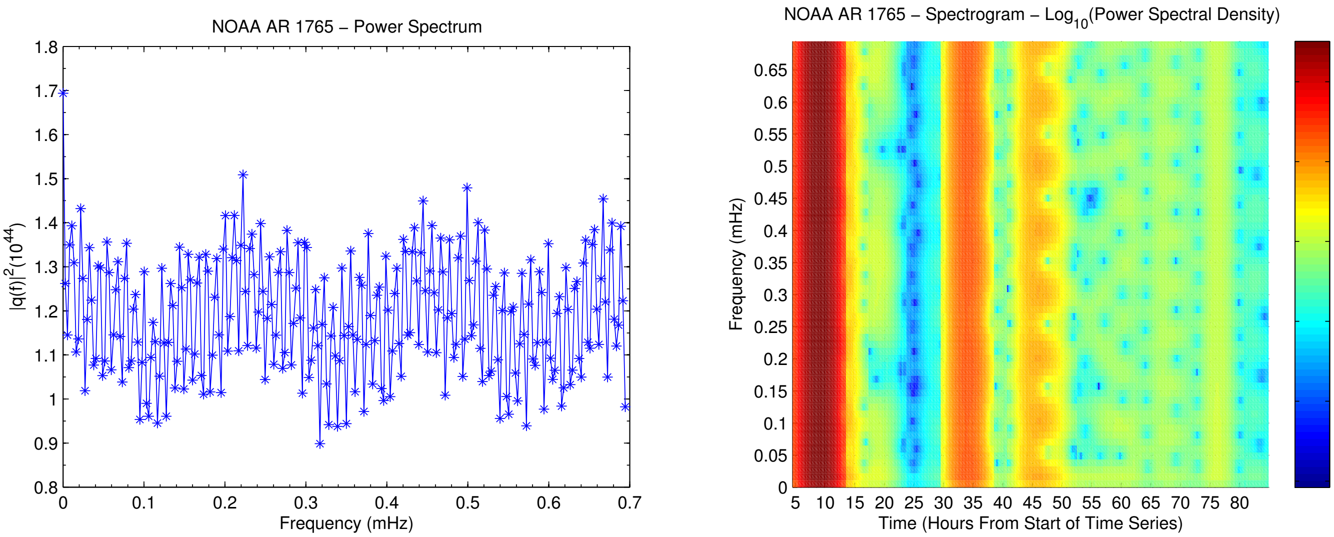

Figure 21: Power Spectrum and Spectrogram for C AR 1765

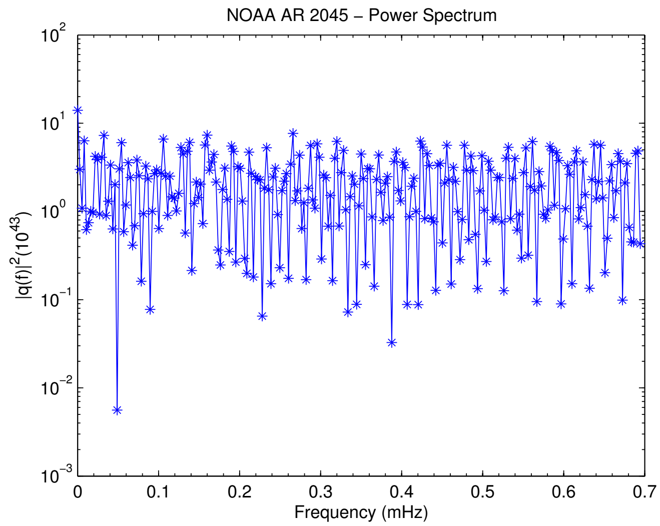

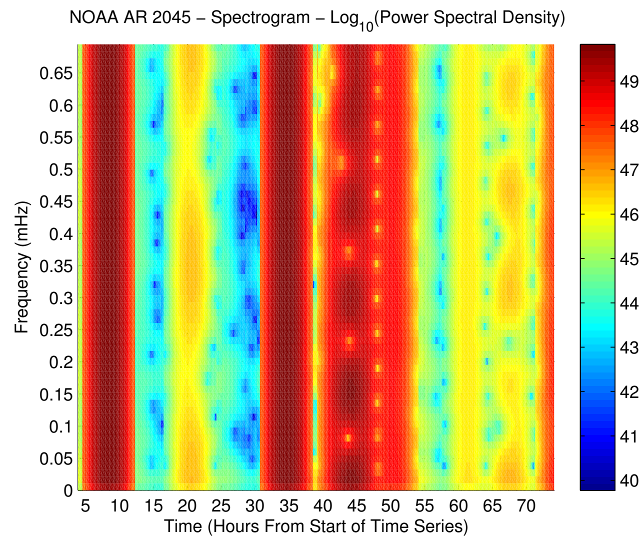

Figure 22: Power Spectrum and Spectrogram for C AR 2045.

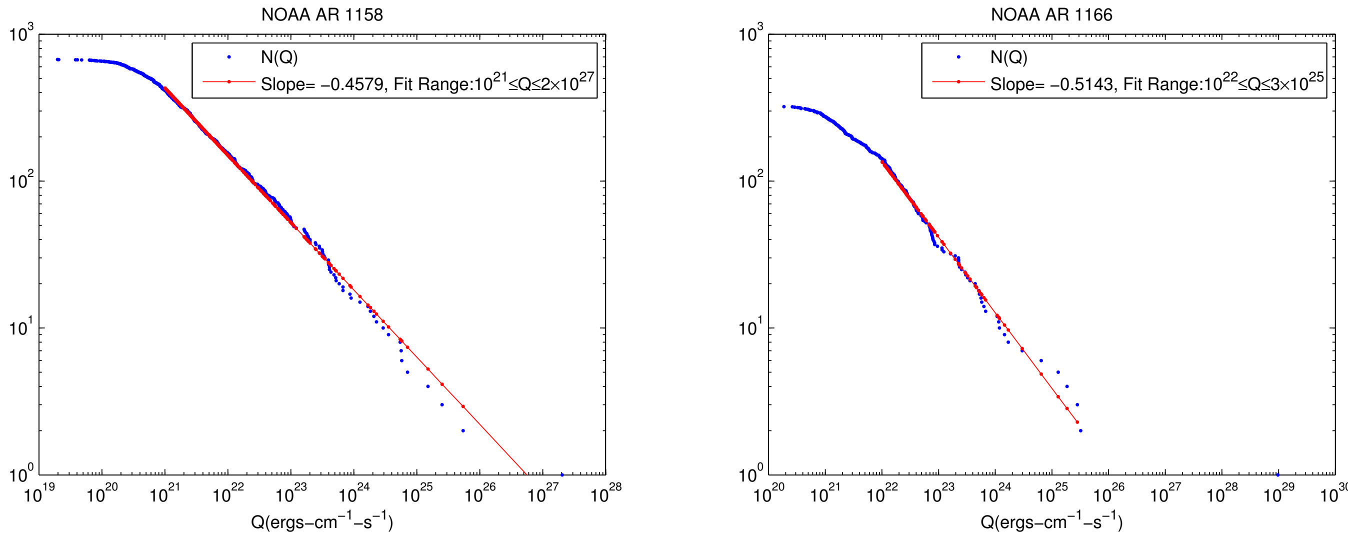

Figure 23: CDFs for SF ARs 1158 and 1166.

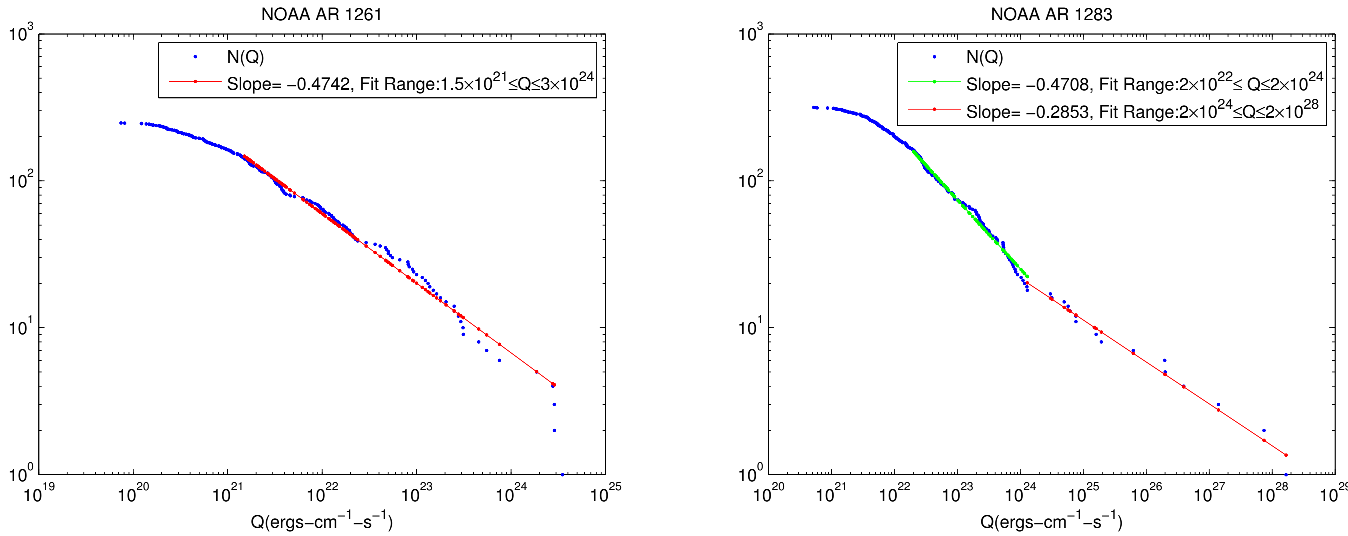

Figure 24: CDFs for SF ARs 1261 and 1283.

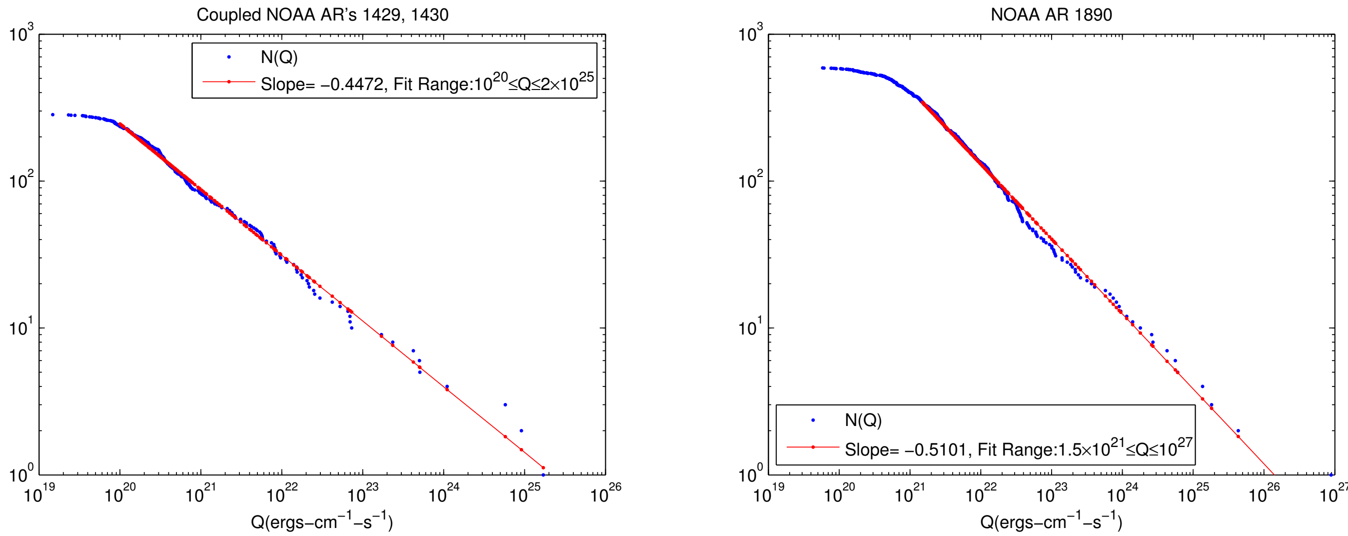

Figure 25: CDFs for SF ARs 1429/1430 (coupled) and 1890.

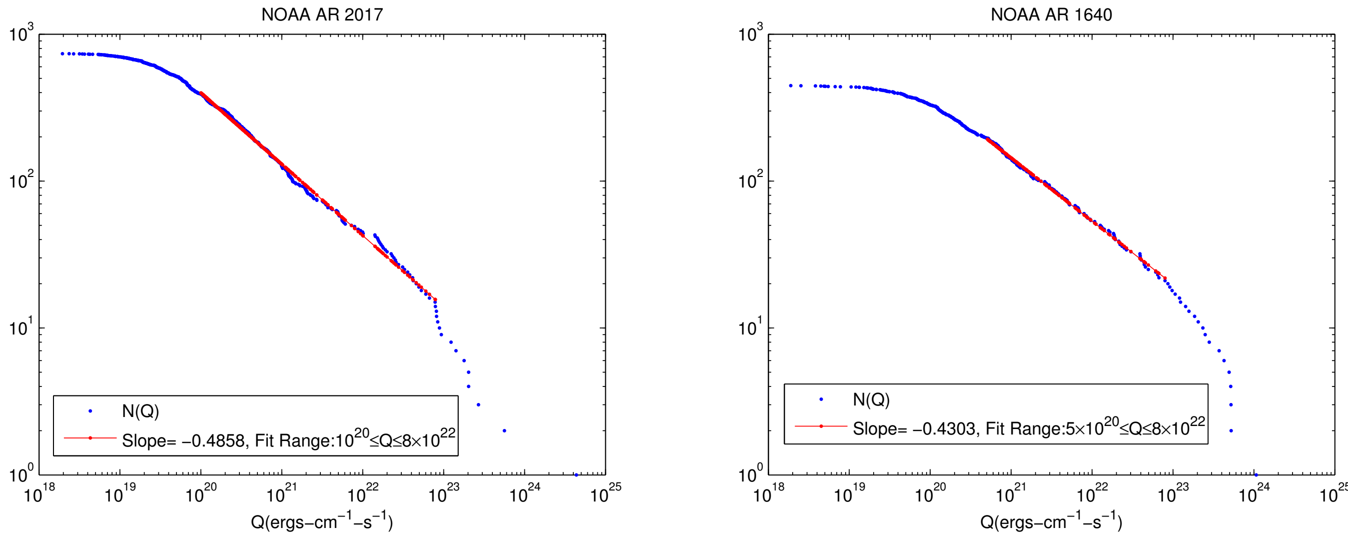

Figure 26: CDFs for SF ARs 2017 and C AR 1640.

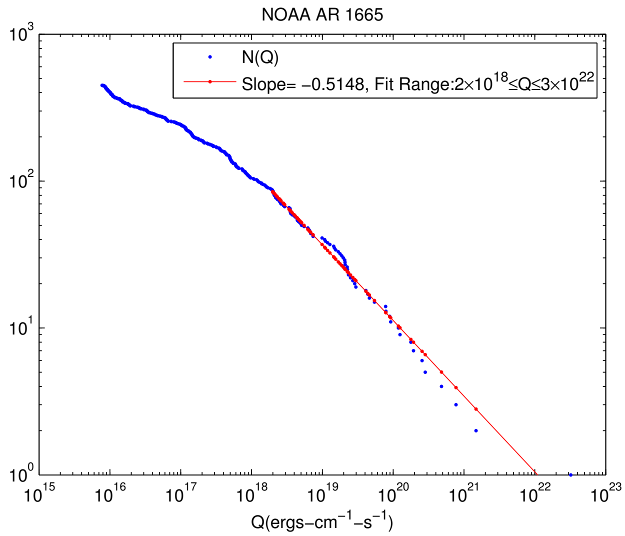

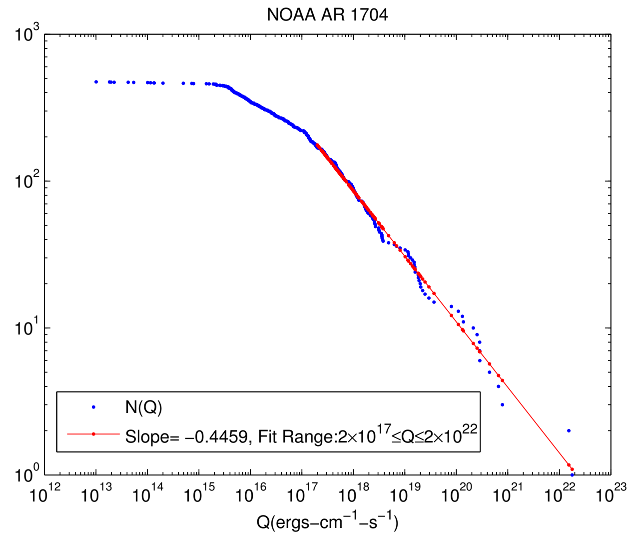

Figure 27: CDFs for C ARs 1665 and 1704.

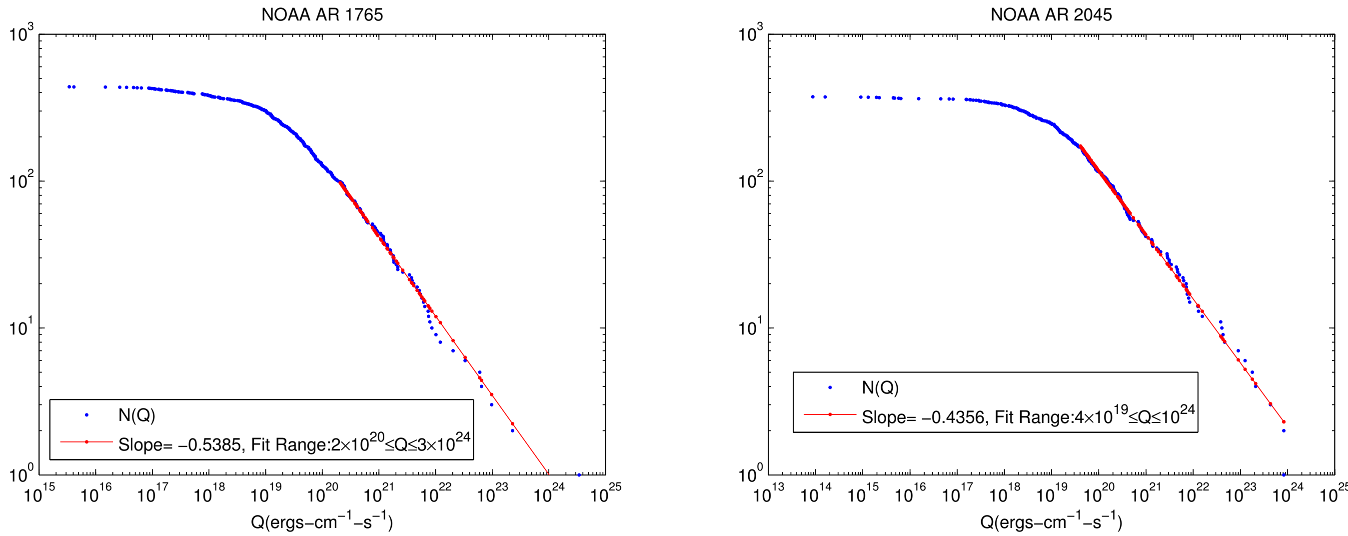

Figure 28: CDFs for C ARs 1765 and 2045.

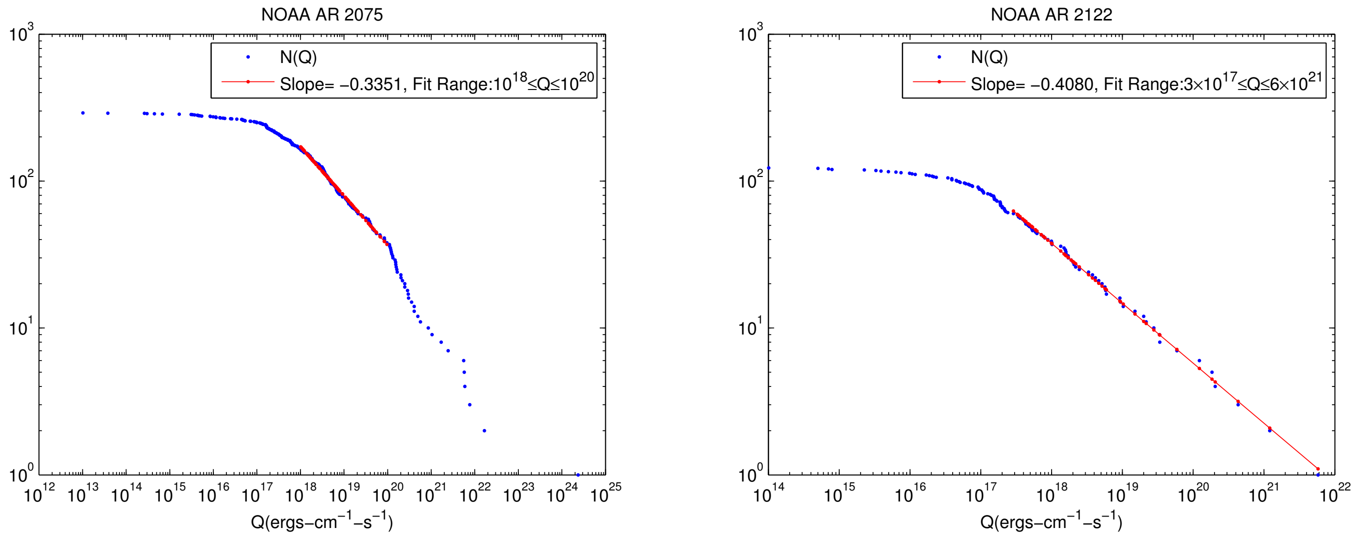

Figure 29: CDFs for CARs 2075 and 2122.

Conclusions

- **There are strong, bursty heating events on granulation scales in the NLR's ARs.**
- **The largest events are convection energy driven, not EM energy driven. Highly non-force-free events ($J_{\perp} \gg J_{\parallel}$).**
- **It is plausible that these events are correlated with M/X flares, preceding them by several hours to several days.**
- **Sample size of 14 ARs is too small to conclude that this apparent correlation is more than plausible.**
- **Analysis of more and longer time series is needed for a definitive statistical test.**